MR. MATHIEU CASTELA (Orcid ID : 0000-0001-8745-9583)

Received Date : 15-Mar-2016

Revised Date : 14-Dec-2016

Accepted Date : 27-Dec-2016

Article type : Regular Article

IGF1R signaling acts on the anagen to catagen transition in the hair cycle

Short title:

IGF1R in bulge cells

Mathieu Castela* [1,2], Fabien Linay* [1,2], Edwige Roy [1,2,3], Philippe Moguelet [4], Jie Xu [1,2], Martin Holzenberger [1,2], Kiarash Khosrotehrani** [3], Selim Aractingi** [1,5,6]

*Authors contributed equally to this work.

**Authors contributed equally to this work and should be considered joint senior authors.

INSTITUTIONS:

1. INSERM UMRS_938, Saint-Antoine Research Center, Paris, France
2. UPMC Université Paris 6, Paris, France
3. The University of Queensland, UQ Centre for Clinical Research, Experimental Dermatology, Group, Brisbane, QLD, Australia.
4. Hôpital Tenon AP-HP, Department of Pathology, Paris, France

5. Université Paris 5 Descartes, Paris, France

6. Hôpital Cochin, AP-HP, Department of Dermatology, Paris, France

7.

CORRESPONDENCE:

Selim Aractingi

INSERM UMRS 938, centre de recherche Saint Antoine, Team Progenitors and endothelial cells during & after pregnancy, 27 rue Chaligny, 75012 Paris, France

Tel: +33140011365 Fax: +33140011423

Email: selim.aractingi@gmail.com

ABSTRACT

Insulin like growth factor 1 (IGF1) is important for skin development and homeostasis. However, overexpression and inactivation studies have produced variable findings regarding its role in hair follicle (HF) biology. Here, we studied a conditional and inducible knockout of the IGF1 receptor (IGF1R) in keratin 15-expressing bulge cells. Deletion of IGF1R after the development of the skin appendages in K15-IGF1R^{KO} mice showed no abnormalities in epidermal homeostasis. Numbers of bulge cells were lower in K15-IGF1R^{KO} mice than in controls, without consequences on wound healing, at least in young mice. K15-IGF1R^{KO} HFs entered anagen phase earlier than controls and showed a delay in the anagen/catagen switch. The expression of BMP-4 mRNA was inhibited in HFs from K15-IGF1R^{KO}. MED1

transcription was impaired in the epidermis of K15-IGF1R^{KO} mice. These findings suggest that IGF1R controls the hair cycle, partly through BMP-4 activation.

KEY WORDS

IGF1R, hair cycle, anagen, stem cells, conditional gene targeting

ABBREVIATIONS

IFE, interfollicular epidermis; HF, hair follicle; IGF1, insulin-like growth factor 1; IGF1R, insulin-like growth factor 1 receptor; IGFBP, insulin-like growth factor binding protein; KO, knockout

INTRODUCTION

Insulin-like growth factor (IGF1) pathway has pleiotropic effects on numerous developmental and post developmental processes. In the skin, IGF1 is implicated in various physiological and pathological phenomenons. Indeed, IGF1 and several high-affinity IGF-binding proteins (IGFBP) are expressed in the hair follicle (HF), suggesting that the IGF signaling pathway regulates the biology of HFs. In particular, IGF1 is expressed in the dermal papilla and dermal fibroblasts (1). Its main receptor, IGF1R, is expressed in the hair epidermis as well as in the dermal papilla. IGF1/IGF1R is needed in normal homeostasis of epidermis (2) as well as for adapted response to UV (3). Several studies have investigated the role of IGF1/IGF1R in hair growth. Mice with a constitutive homozygous deletion of IGF1R die soon after birth but show smaller and fewer HFs than wild type mice (4). *In vitro,* IGF-I stimulates HF growth by preventing the HF from entering a catagen-like state (5). In accordance, in rats, transcript levels of IGF1R are high in HFs in the anagen phase (6).

However, other studies report inconsistent findings. Rudman (7) found that IGF1R expression in human hair was restricted to the epithelial layers of differentiated hair but was absent from bulge proliferative cells, suggesting that IGF1 acts there only as a morphogen (7). Furthermore, excessive PI3K activation in SGK3^{KO} mice, which mimics constitutive IGF1R signaling, leads to premature entry into the catagen phase (8). Overexpression of IGF1 under the control of involucrin or K14 promoter leads to defects in zigzag hairs and modifies the hair cycle (9, 10). K14 transgenic IGF1 mice show a prolonged anagen 1 phase (9). When the expression of transgenic IGF1 is driven by the involucrin promoter, the re-initiation of a new anagen phase is delayed (10). Mice with conditional inactivation of IGF1R in K14-expressing cells were generated by Stachelscheid *et al.* (2). Interestingly, the authors report that the abundance of K15 protein and the number of label-retaining stem cells was low in these mice because of altered IGF1R signaling (2). In this study, the deletion of IGF1R was constitutive in the entire K14 lineage, which encompasses most of the basal layer of the skin and pilosebaceous unit. Therefore~~,~~ the consequences of inactivating IGF1R signaling specifically in the hair bulge compartment remain unclear. To address the precise role of IGF1R in the hair cycle in adults, we developed an inducible murine model of IGF1R deletion restricted to K15^{+} cells. We show here that IGF1R signaling regulates entry into the hair cycle, possibly through interaction with BMP-4.

MATERIALS AND METHODS

Mice: We generated mutant mice lacking IGF1R in HF stem cells. For this we used the Krt1-15-CrePR1 mouse strain (11) obtained from Jackson Laboratories (B6;SJL-Tg(Krt1-15-cre/PGR)22Cot/J) and crossed them to 129/Sv IGF1R$^{LOX/LOX}$ mice (12). We thereby obtained Krt1-15-CrePR1;IGF1R$^{LOX/LOX}$ mice. Since, our floxed allele had a neo cassette shown to be hypomorphic we used as controls WT mice with identical genetic background. Council guidelines and approved by our Institutional Animal Care and Use Committee (approval number #5620).

Genotyping: Krt1-15-CrePR1;IGF1R$^{LOX/LOX}$ mice were genotyped for IGF1R by using multiplex assay (13) (PCR primer sequences in Table S1)

Induction: Krt1-15-CrePR1;IGF1R$^{LOX/LOX}$ and WT mice were shaved and topically treated with RU486 (Sigma-Aldrich) on their dorsal skin during telogen once a day for 5 consecutive days at 3 weeks of age. RU486 was formulated in solution of 10% ethanol and 90% sunflower oil (Sigma-Aldrich), and 200 µl of this solution was applied to the dorsal skin of KO mice and WT mice.

Flow cytometry: Back skin was shaved and harvested 10 days after induction and incubated overnight at 4°C in 0.05% trypsin-EDTA 1X (Invitrogen) for mechanical separation of the epidermis. The epidermis was then digested in the same buffer for 15 min at 37°C and filtered using a 100 µm cell strainer (BD Pharmingen) to obtain a single cell suspension. Plucked hairs were digested 60 min at 37°C in collagenase A (Roche) and then filtered using a 100 µm cell strainer (BD Pharmingen) to obtain a single cell suspension. Antibodies used for cytometry were CD34-eFluor660 (1:100; eBioscience) and CD49f-PE (1:100; eBioscience). Flow cytometry data was acquired using a BD FACSCALIBUR cytometer (BD Pharmingen), cell sorting was performed on a MOFLO Astrios (Beckman Coulter) and subsequently analyzed with FlowJo software (Ashlan). The analysis and the selection of the gate were made in accordance to Nowak protocols (14).

Immunostaining: 5 µm cryosections from frozen tissue or microtome sections from embedded paraffin were obtained. After permeabilization with Triton X-100, sections were blocked using 20% normal goat serum (DakoCytomation). Primary antibodies: rabbit anti-human/mouse Loricrin (1:800; Covance), rabbit anti-human/mouse filaggrin (1:200; Covance), rabbit anti-Keratin 14 (1:500; Covance), rabbit anti-human/mouse Ki67 (1:100; Novocastra Leica), rat anti-mouse CD34 (1:50; Abcam). We used secondary antibodies goat anti-rabbit IgG labeled with Cy3 and donkey anti-rat IgG labeled with Alexa 488 (1:1000; Invitrogen). Slides were counterstained with 0.3 µg/ml DAPI (Sigma-Aldrich). For immunohistochemistry, signal was detected using the Vectastain ABC Elite Mouse/Rabbit/Goat IgG detection kit (Vector Laboratories) following the manufacturer's protocol.

Microscopy, scoring and measurements: We used Nikon Eclipse 90i fluorescent microscope equipped with Nikon DS-Fi1C digital camera (Nikon). For cell scoring, photographs of 3 different fields of the different skin regions (epidermis, dermis, hypodermis and HF) were taken, and labeled cells were counted and reported as percentage of total nuclei. Mean percentage of labeled cells was calculated for each specimen. Measurements were done using ImageJ software (NIH).

RNA extraction and quantitative PCR: Total RNA was extracted from full skin or plucked hair or sorted cells using the RNeasy total RNA Mini kit (Qiagen). Total RNA (1 μg) was reverse transcribed using high capacity cDNA reverse transcription kit (Applied Biosystems). Real-time PCR was conducted using SYBRGREENPCR Master Mix (Applied Biosystems) on ABI Prism 7300 (Applied Biosystems). mRNA values were normalized to the expression level of 18S rRNA. Primer sequences are in Table S1. Each sample was analyzed in duplicate.

Surgical wounds: Mice were anesthetized by inhalation of 4.9% isofluorane (Aerane, Baxter) at 300 ml/min ambient air flow. After depilation, 5 mm surgical wounds were generated using a punch biopsy device. All tissues above the *panniculus carnosus* were excised. Wounds were left uncovered until they were harvested. Standardized pictures of the wounds were taken on different time points using a Sony Cybershot 10.1 megapixels DSC-W180 digital camera (Sony). Wound tissues were harvested either snap-frozen in liquid nitrogen and stored at -80°C.

Proteins extraction and western blot: Fresh tissues from telogen dorsal skin were disrupted into liquid nitrogen and resuspended into RIPA buffer (Biorad). Equal amounts of the extracted proteins (20 μg) were resolved using NuPAGE 4-12% Bis-Tris Gel (Novex, Invitrogen) and transferred to nitrocellulose membrane (GE Healthcare). The membranes were incubated with antibodies directed against TRAP220/MED1 (phospho T1457) and TRAP220/MED1 (1:300; rabbit polyclonal; Abcam), phospho-Smad2 (Ser465/467), IGF-1 receptor β and β-Actin (1:1,000; 1:500; & 1:2,000; rabbit polyclonal; Cell Signaling), and phospho-Smad1/5/8 (Ser463/465) (1:500; rabbit polyclonal; Millipore). After this incubation, membranes were incubated with anti-rabbit HRP-conjugated

antibody (1:2,500; Cell Signaling). We treated the membranes with ECL prime (GE Healthcare) and signals were captured on ChemiDoc (Biorad). Protein bands were analyzed by densitometry with ImageJ.

Hair cycle analysis: To achieve a synchronized anagen development over the whole back skin area, hair shafts of the back fur coat of mice with all follicles in telogen (pink skin) were depilated using a cold wax strip (VEET Ready-to-use Wax Strips). The procedure was performed under isofluorane anesthesia, at the same day for WT and KO mice, namely 4-weeks after topical application of mifepristone. Standardized pictures of the back skin were taken every 2 or 3 days using a Sony Cybershot 10.1 megapixel DSC-W180 digital camera (Sony).

Statistical analysis: Data were expressed as means ± SEM. Means between 2 groups were compared using the Mann Whitney test. $p < 0.05$ was considered to be statistically significant.

RESULTS

K15-IGF1R^{KO} conditional knockout mice display low levels of IGF1R

We generated mutant K15-IGF1R^{KO} mice in a 129/SvPas × C57BL/6J genetic background using homozygous floxed IGF1R exon 3 and mifepristone-inducible Cre recombinase expressed from the K15 promoter. WT and KO were treated at 3 weeks of age with mifepristone, after the completion of hair morphogenesis. Topical applications of mifepristone induced efficient deletion of IGF1R (Fig. S1a). KO induction did not affect body weight at week 5 suggesting no systemic IGF1R inactivation (Fig. S2a). One week post-induction, IGF1R mRNA levels in the skin samples were 50% lower in K15-IGF1R^{KO} than in control mice (Fig. S1b). To examine more selectively the K15 progeny, we cell sorted epidermis populations and harvested plucked hair. IGF1R mRNA levels in CD34^{+}α6-integrin^{high} bulge cells and plucked hairs were respectively 81.6% and 70% lower in K15-IGF1R^{KO} mice than in control littermates ($p = 0.0028$; $p = 0.014$), indicating that IGF1R was efficiently inactivated in K15-IGF1R^{KO}

mice (Fig. S1c and Fig. S3). The abundance of IGF1R protein in whole skin was 60% lower in K15-IGF1R^{KO} than in WT mice (p = 0.029) (Fig. S1d). Finally, IGF1R immunostaining showed an absence of IGF1R protein expression in bulge area in K15-IGF1R^{KO} mice (Fig. S1e).

Morphology, proliferation and differentiation of the epidermis are unaffected in K15-IGF1R^{KO} mice

Histopathological analysis of K15-IGF1R^{KO} mice did not show any skin alterations. Indeed, the morphology and thickness of the epidermis and dermis were similar in K15-IGF1R^{KO} mice and WT controls (Fig. S1f,h) at all HF stages. However, the hypodermis compartment was thicker during catagen phase in KO mice (p < 0.0001) (Fig. S1h and Fig. S4a). We observed in IGF1R KO mice an increase in the number of adipocytes (p = 0.0066) while the cell surface remained unchanged (Fig. S4b). Epidermal proliferation (Fig. S2b) and hair density were also comparable between K15-IGF1R^{KO} and control mice (Fig. S1g). We used loricrin and filaggrin as markers to analyze epidermal differentiation but found no differences between K15-IGF1R^{KO} mice and controls (Fig. S5).

We made excisional wounds 10 days after induction on the back of K15-IGF1R^{KO} and control mice and monitored kinetics of wound healing (Fig. S6a). Surface morphometry showed that there was no delay in wound closure in K15-IGF1R^{KO} mice (Fig. S6b).

The adult epidermal hair bulge-niche is influenced by IGF1R deletion

To study the epidermal compartment and its stem cells, we analyzed keratinocyte suspensions by flow cytometry (14). Ten days after KO induction, when K15-IGF1R^{KO} and controls were in anagen phase, numbers of CD34^{+}α6-integrin^{high} bulge cells were substantially lower in K15-IGF1R^{KO} than in controls (1.6 ± 0.6% versus 4.2 ± 1.3%, respectively; p < 0.005, Fig. 1a,b). Interestingly, the number of suprabasal cells was unaffected, which again evokes the specificity of the inactivation of IGF1R in our

model in HF (Fig. 1a,b). In contrast, interfollicular epidermis (IFE) non-bulge cells population was also affected by the inactivation of IGF1R. Indeed after induction IFE non-bulge cells decreased of 49% (Fig. 1a,b). The number of $CD34^+$ labelled located in the bulge was measured. There was a decrease of bulge $CD34^+$ cells in K15-IGF1R^{KO} compared to control mice (p = 0.0047, Fig. 1c), confirming our FACS results. Immunostaining of K15 demonstrated a depletion of $K15^+$ cells in bulge area (Fig. 1d). We also measured K15 mRNA levels know to correlate with bulge ~~stem~~ cell compartment (15), from plucked hairs in the telogen phase. K15 transcript levels were lower in K15-IGF1R^{KO} than in WT mice, demonstrating depletion of bulge ~~stem~~ cells in K15-IGF1R^{KO} mice (Fig. 1e and Fig. S7).

K15-IGF1R^{KO} hair follicles show early entry into anagen phase and a delay in anagen/catagen switch

We followed the two first hair cycles in K15-IGF1R^{KO} mice starting from induction (P21) (Fig. 2a). The stages of the hair cycle were determined by the color of dorsal skin (16). WT and K15-IGF1R^{KO} mice showed no obvious differences in the first cycle after mifepristone induction. In addition, K15-IGF1R^{KO} HFs entered the anagen phase earlier than those of WT mice, in the absence of any anagen-inducing stimuli (p = 0.0001; Fig. 2b,c). Histological analysis showed that at P51, most hairs in K15-IGF1R^{KO} mice were in the anagen stage whereas control mice were in telogen stage at the same date (Fig. 2d). To refine monitoring of the hair cycle, we synchronized hair growth by wax depilation 4-weeks after topical application of mifepristone (17) (Fig. 3a,b). HFs entered the anagen stage at exactly the same age in both groups and the mice showed no differences in hair cycle phase, whether assessed by dorsal skin color or histological evaluation (D12; Fig. 3b,d). When control mice were entering catagen phase, K15-IGF1R^{KO} mice still displayed anagen growth with large pigmented areas on their back skin (p = 0.041, D20; Fig. 3b,c). Histological analysis at this late point (D20 after wax depilation) from the back of the dorsal skin revealed large differences in hair stages between KO and control groups (Fig. 3d). Indeed, 22.8 ± 2.3% of HFs in K15-IGF1R^{KO} mice were still in the anagen

phase, compared to only 3.4 ± 1.9% in control mice (p = 0.003; Fig. 3f). We searched for alterations in hair type but found no differences, which we expected since KO induction was performed after morphogenesis (Fig. 3e). In particular, KO and control groups displayed similar proportion of zigzag hairs.

IGF1R regulates the anagen phase by affecting the ~~stem~~ cell bulge and hair follicle cycle with activation of BMP-4 and MED1

BMP and their inhibitors play a major role in the activation of each hair cycle step (18). In addition, studies have shown that several molecules such as TGFβ, BMP, WNT, DKK, SFRP, WIF as well as SHH and Notch are implicated in the maintenance and/or regeneration of hair follicles (19). To understand the origin of HF cycle abnormalities in K15-IGF1R^{KO} mice, we chose to evaluate number of these signals. We used plucked hairs from the first telogen phase after induction of K15-IGF1R^{KO} and control mice. The abundance of c-Myc, NT3, FGF5, Sox9 and BMP-2 mRNA was similar between the two groups (Fig. S9a and Fig. S10). BMP-4 mRNA levels were 70% lower in K15-IGF1R^{KO} than in control mice (p = 0.008; Fig. S9a). TGFβ2, SHH and PTCH1 mRNA levels were respectively 6-fold, 20-fold and 3-fold higher in K15-IGF1R^{KO} mice than in controls (Fig. S9c). Using western blotting on whole epidermis, phospho-Smad2 was accordingly higher in these mice than in controls (p = 0.038, Fig. S9d), while the abundance of phospho-Smad1/5/8 was similar, possibly because the BMP-2 pathway was not impacted by IGF1R KO (Fig. S9b). MED1 expression has been shown to play a crucial role in hair cycling [26]. We found that both the expression and phosphorylation of MED1 were lower in K15-IGF1R^{KO} than in control mice (Fig. 4).

DISCUSSION

Mesenchymal epidermal interactions are important for HF morphogenesis and cycling. IGF1 has many roles in development and is expressed in the mesenchymal compartment of the HF whereas the expression of its receptor is more widespread. To explore the potential role of IGF1 signaling in this process, we developed an inducible murine model to inactivate IGF1R in keratin-15-expressing cells after HF development. In these mice, IGF1R mRNA levels were low specifically in HF cells, indicating that IGFR1 was selectively inactivated in the progeny of hair bulge cells and confirmed by immunostaining. Despite a decrease in IFE non-bulge cells, that may relate to the fact that $K15^+$ progeny colonize also IFE, epidermal proliferation and differentiation were unaffected by IGF1R depletion even during wound healing process. However, in our transgenic mice, the pool of $CD34^+$ bulge ~~stem~~ cells was low and the hair cycle was characterized by earlier entrance into hair cycle as well as a prolonged anagen stage. Inactivation of IGF1R impaired the expression of BMP-4 and MED1 in the HF, which are negative regulators of hair cycling (20, 21), and thus inhibited downstream signaling by these factors.

We have used original mutant mice where IGF1R was deleted in the $K15^+$ cells. Such inactivation was demonstrated through PCR on plucked hair cells, using western blot and immunostaining. Indeed, since $K15^+$ cells are a small portion of the whole epidermis (5%) (11), full skin or even full epidermal analysis could not be used to precisely assess the depletion of IGF1R in this compartment. Therefore, we chose to study the cells obtained after plucking the hairs. Indeed such technique, harvest only the lower part of the hair follicle as shown in post plucking sections (Fig. S7 and Fig. S8) without contamination by the IFE population. While, Hsu *et al.* have shown that, the majority of $CD34^+$ hair follicle cells remain attached to the bulge after plucking (22), our FACS analysis of the hair plucked cells indicates that this technique led to a considerable enrichment in the $CD34^+\alpha6\text{-integrin}^{high}$ bulge cells. Therefore, we consider that it is a useful tool to assess the changes in the expression of any gene in bulge cells. It allowed us to depict that nearly 70% of IGF1R expression was absent in the

plucked cells after induction. These results are very close to the 81.9% decrease in IGF1R^{+} in the sorted bulge population confirming the usefulness of plucked hairs.

Using FACS done at the same day of hair cycle, we showed that the compartment of hair bulge cells co-expressing CD34 and α6-integrin was smaller in transgenic than in control mice. Of note, other compartments in the HF were not affected. These markers identify stem cells within the HF as shown by the proliferation capacity of these cells in clonogenic assays and their multi-lineage potential upon transplantation (14, 23, 24). We also counted CD34^{+} cells in the bulge and found 4.5 times fewer cells in K15-IGF1R^{KO} than in control mice, as predicted by FACS. Finally, K15 mRNA levels were also 60% lower in KO than in control mice in cells from plucked hairs. Therefore, all these results strongly suggest that adult bulge ~~stem~~ cells depend on IGF1R signaling. Mice with constitutive ubiquitous inactivation of the IGF1R display smaller and fewer HFs than wild type mice, implying a role for IGF1 signaling in HF development (4); however, our study shows for the first time that IGF1R also regulates the biology of bulge cells post-developmentally. Indeed, in the study of Liu *et al*. (4) stem cells may have been affected by developmental processes, whereas we examined the function of IGF1R after the normal formation of HFs and their bulge, and show that IGF1R is important for the maintenance of the CD34^{+}α6-integrin^{high} population of adult stem cells. Of note, dermal fibroblasts, including dermal papilla cells, secrete IGF1 (10). The precise mechanisms of reduced bulge cells in KO mice, such as exhaustion or apoptosis, were not addressed in this study.

Of note, IFE compartment was affected by IGF1R inactivation (Fig. S11). Indeed, K15-CrePR1 can seed the basal layer of IFE non-bulge cells, mainly in non homeostatic conditions (11). IGF1/IGF1R pathway is known to play a role in the regulation of epidermal proliferation (2) and wound healing (25). In our model, we found that despite a partial decrease of the IFE non-bulge cells population, induced by the inactivation of IGF1R under the control of the K15 promoter, there was no impact on the skin epidermal thickness and healing. This result probably relies on the fact that the decrease in the K15 cellular progeny was too low to influence significantly epidermal repair.

Previous work showed that in the absence of IGFs, HFs *in vitro* undergo an anagen to catagen transition (5). In contrast, other authors showed that overexpression of IGF1 in $K14^{+}$ cells accelerates anagen phase and impairs the anagen-catagen transition (9). In our *in vivo* model, we found earlier entrance in hair cycle as well as prolonged anagen phase in K15-expressing cells lacking IGF1R consistent with the results by Semenova *et al*. (9). This result indicates that IGF1/IGF1R is needed for the switch to the catagen stage. Of note, the only previous *in vivo* study analyzing the role of IGF1 in HFs involved the overexpression of IGF1 in keratinocytes (10). This may not reflect the situation *in vivo* because IGF1 is also produced by dermal cells and the dermal papilla (10). Of note, since IGF1R inactivation was performed after HF morphogenesis, the distribution of hair types was unaffected in our post developmental K15-$IGF1R^{KO}$ mice. Thus, in adult mice, the IGF1/IGF1R pathway affects the number/activation of hair bulge ~~stem~~ cells, influences the hair cycle entrance and also delays catagen entry.

An increase in thickness of the hypodermis during catagen phase in K15-$IGF1R^{KO}$ was found. The number of adipocytes was increased in our KO mice without change in their surface. Adipocytes are known to influences hair follicle stem cells (26, 27). Our data evoke a reverse relationship where prolonged anagen phase leads to proliferation of adipocytes, these effects persisting in catagen phase However, in a study of Kwack *et al.* where anagen phase was prolonged; hypodermis at catagen phase seemed also thickened (28).

Stachelscheid *et al.* addressed the role of IGF1R *in vivo* in the epidermis (2). This group has developed constitutive $IGF1R^{KO}$ mice in the Keratin 14 (K14) lineage. Using colony forming assay and label retaining cells, these authors showed that IGF1R is crucial for the maintenance of the epidermal progenitor pool (2). In addition, they demonstrated that K14-IGF1R played a role in $K15^{+}$ cell survival in IFE and HF through Rac activation during morphogenesis. In our model, there were no changes in thickness of the epidermis, nor the dermis. This probably relates to the fact that IGF1R

was inactivated in bulge cells from HF after morphogenesis and that we analyzed steady state conditions in young mice.

IGF-1R KO inhibits Rac that up-regulates c-Myc (29). This molecule itself controls negatively the numbers of progenitor cells in the IFE (30, 31). In our mouse model, c-Myc expression level was not modified. Therefore, IGF1R signaling could signal independently from Rac in the K15 lineage. Alternatively, the IGF1R KO in adult mice could lead to different pathway changes. Several molecules are implicated in checkpoints of the hair cycle including BMPs, TGFβ, SHH, FGF and MED1. In our K15-IGF1R^{KO} mice, there were high levels of SHH, PTCH receptor and TGFβ2 RNA. The strong expression of SHH/PTCH probably results from a regulatory phenomenon secondary to IGF1R inactivation (32). Our K15-IGF1R^{KO} mice also showed low levels of BMP-4 mRNA, which is unlikely to result from MED1 inhibition (33). Of note, dermal BMP-2 and -4 inhibitions through *noggin* leads to hair cycle entrance (34). This is in accordance with our observations. We also evaluated MED1 since it may regulate the hair cycle (20, 33). Both MED1 transcript levels and the abundance of phospho-MED1 were significantly lower in K15-IGF1R^{KO} than in control mice. Besides other genes, phosphorylated MED1 regulates, among other genes, the transcription of BMP-2, SHH, PTCH1 and TGFβ1 (20). MED1 inactivation in the K14 lineage in mice leads to hair loss and the accelerated and sustained activation of anagen phase in the post-morphogenic cycle (20). Mice with a constitutive K5-MED1^{KO} deletion show a smaller bulge compartment and increased entry in hair cycle (33). Similitudes in the phenotype between IGF1R and MED1^{KO} mice suggest a mutual interaction between these molecules.

Our results have limitations. The first one is the incomplete efficiency of Cre/lox deletion in our mice that may have prevented a clearer phenotype. In addition, we could not fully demonstrate functional alterations of bulge ~~stem~~ cells upon IGF1R inactivation. Nevertheless, our findings indicate the importance of postnatal IGF1/IGF1R signaling in the anagen-catagen switch in the HF cycle. Despite the depletion of this important factor in Keratin 15 positive cells, the skin is able to

compensate in steady state conditions. In addition, the loss of IGF1R in K15-expressing cells results in HF cycle abnormalities, which appear to be mediated through various signals, including BMP-4.

ACKNOWLEDGEMENTS

We thank Michele Oster, Sylvie Annie Munier (FACS department UMS30), and Tatiana Ledent Saint Antoine Research Center) for expert contributions. MH and JX contributed essential materials. MC, FL and ER performed experiments on K15 IGF1R mice. MH, KK and SA designed and conducted the research study. MC, FL, ER, MH, KK and SA wrote the paper.

FUNDING

This work was supported by ANR Physio Homeoderm granted to KK and MH, and Société Française de Dermatologie (SFD). Fabien Linay received support from French Ministry for Education (MEN) and Association pour la Recherche sur le Cancer (ARC). Mathieu Castela received an MEN fellowship.

REFERENCES

1. Zhao J, Harada N, Kurihara H, et al. Dietary isoflavone increases insulin-like growth factor-I production, thereby promoting hair growth in mice. J Nutr Biochem 2011: 22: 227-233.

2. Stachelscheid H, Ibrahim H, Koch L, et al. Epidermal insulin/IGF-1 signalling control interfollicular morphogenesis and proliferative potential through Rac activation. The EMBO journal 2008: 27: 2091-2101.

3. Thumiger S P, Adams T E, Werther G A, et al. UV induced responses of the human epidermal IGF system: impaired anti-apoptotic effects of IGF-I in HaCaT keratinocytes. Growth Factors 2005: 23: 151-159.

4. Liu J P, Baker J, Perkins A S, et al. Mice carrying null mutations of the genes encoding insulin-like growth factor I (Igf-1) and type 1 IGF receptor (Igf1r). Cell 1993: 75: 59-72.

5. Philpott M P, Sanders D A, Kealey T. Effects of insulin and insulin-like growth factors on cultured human hair follicles: IGF-I at physiologic concentrations is an important regulator of hair follicle growth in vitro. J Invest Dermatol 1994: 102: 857-861.

6. Little J C, Westgate G E, Evans A, et al. Cytokine gene expression in intact anagen rat hair follicles. J Invest Dermatol 1994: 103: 715-720.

7. Rudman S M, Philpott M P, Thomas G A, et al. The role of IGF-I in human skin and its appendages: morphogen as well as mitogen? J Invest Dermatol 1997: 109: 770-777.

8. Alonso L, Okada H, Pasolli H A, et al. Sgk3 links growth factor signaling to maintenance of progenitor cells in the hair follicle. J Cell Biol 2005: 170: 559-570.

9. Semenova E, Koegel H, Hasse S, et al. Overexpression of mIGF-1 in keratinocytes improves wound healing and accelerates hair follicle formation and cycling in mice. Am J Pathol 2008: 173: 1295-1310.

10. Weger N, Schlake T. Igf-I signalling controls the hair growth cycle and the differentiation of hair shafts. J Invest Dermatol 2005: 125: 873-882.

11. Morris R J, Liu Y, Marles L, et al. Capturing and profiling adult hair follicle stem cells. Nat Biotechnol 2004: 22: 411-417.

12. Holzenberger M, Leneuve P, Hamard G, et al. A targeted partial invalidation of the insulin-like growth factor I receptor gene in mice causes a postnatal growth deficit. Endocrinology 2000: 141: 2557-2566.

13. Leneuve P, Zaoui R, Monget P, et al. Genotyping of Cre-lox mice and detection of tissue-specific recombination by multiplex PCR. Biotechniques 2001: 31: 1156-1160, 1162.

14. Nowak J A, Fuchs E. Isolation and culture of epithelial stem cells. Methods Mol Biol 2009: 482: 215-232.

15. Liu Y, Lyle S, Yang Z, et al. Keratin 15 promoter targets putative epithelial stem cells in the hair follicle bulge. J Invest Dermatol 2003: 121: 963-968.

16. Muller-Rover S, Handjiski B, van der Veen C, et al. A comprehensive guide for the accurate classification of murine hair follicles in distinct hair cycle stages. J Invest Dermatol 2001: 117: 3-15.

17. Paus R, Stenn K S, Link R E. Telogen skin contains an inhibitor of hair growth. Br J Dermatol 1990: 122: 777-784.

18. Jamora C, DasGupta R, Kocieniewski P, et al. Links between signal transduction, transcription and adhesion in epithelial bud development. Nature 2003: 422: 317-322.

19. Li L, Xie T. Stem cell niche: structure and function. Annu Rev Cell Dev Biol 2005: 21: 605-631.

20. Oda Y, Hu L, Bul V, et al. Coactivator MED1 ablation in keratinocytes results in hair-cycling defects and epidermal alterations. J Invest Dermatol 2012: 132: 1075-1083.

21. Oshimori N, Fuchs E. Paracrine TGF-beta signaling counterbalances BMP-mediated repression in hair follicle stem cell activation. Cell Stem Cell 2012: 10: 63-75.

22. Hsu Y C, Pasolli H A, Fuchs E. Dynamics between stem cells, niche, and progeny in the hair follicle. Cell 2011: 144: 92-105.

23. Blanpain C, Lowry W E, Geoghegan A, et al. Self-renewal, multipotency, and the existence of two cell populations within an epithelial stem cell niche. Cell 2004: 118: 635-648.

24. Trempus C S, Morris R J, Bortner C D, et al. Enrichment for living murine keratinocytes from the hair follicle bulge with the cell surface marker CD34. J Invest Dermatol 2003: 120: 501-511.

25. Etheredge L, Kane B P, Hassell J R. The effect of growth factor signaling on keratocytes in vitro and its relationship to the phases of stromal wound repair. Invest Ophthalmol Vis Sci 2009: 50: 3128-3136.

26. Yang C C, Sheu H M, Chung P L, et al. Leptin of dermal adipose tissue is differentially expressed during the hair cycle and contributes to adipocyte-mediated growth inhibition of anagen-phase vibrissa hair. Exp Dermatol 2015: 24: 57-60.

27. Schmidt B, Horsley V. Unravelling hair follicle-adipocyte communication. Exp Dermatol 2012: 21: 827-830.

28. Kwack M H, Kang B M, Kim M K, et al. Minoxidil activates beta-catenin pathway in human dermal papilla cells: a possible explanation for its anagen prolongation effect. J Dermatol Sci 2011: 62: 154-159.

29. Benitah S A, Frye M, Glogauer M, et al. Stem cell depletion through epidermal deletion of Rac1. Science 2005: 309: 933-935.

30. Arnold I, Watt F M. c-Myc activation in transgenic mouse epidermis results in mobilization of stem cells and differentiation of their progeny. Curr Biol 2001: 11: 558-568.

31. Waikel R L, Kawachi Y, Waikel P A, et al. Deregulated expression of c-Myc depletes epidermal stem cells. Nat Genet 2001: 28: 165-168.

32. Malaguarnera R, Belfiore A. The emerging role of insulin and insulin-like growth factor signaling in cancer stem cells. Front Endocrinol (Lausanne) 2014: 5: 10.

33. Nakajima T, Inui S, Fushimi T, et al. Roles of MED1 in quiescence of hair follicle stem cells and maintenance of normal hair cycling. J Invest Dermatol 2013: 133: 354-360.

34. Kobielak K, Pasolli H A, Alonso L, et al. Defining BMP functions in the hair follicle by conditional ablation of BMP receptor IA. J Cell Biol 2003: 163: 609-623.

FIGURE LEGENDS

Figure 1: Bulge cells are reduced after IGF1R^{KO}. (a) FACS analysis from whole epidermis cell suspension. Representative dot plots from WT and KO mice. (b) Quantification of bulge, suprabasal and IFE non-bulge cells populations in percent of total cells (n = 9 vs 6). (c) Representative histology of skin sections stained for CD34 (positive cells are shown by white arrow head) (n = 3 vs 3). Quantification of CD34^{+} labeling intensity in the bulge aera (n = 3 vs 3). (d) Representative histology of skin sections stained for K15 (white stars show the absence of K15 staining in bulge area) (n = 3 vs 3). (e) K15 mRNA level in telogen phase (n = 6 vs 4). Scale bars: 50 µm on all micrographs. Mann-Whitney test, *$p < 0.05$; mean ± SEM.

Figure 2: Hair cycle in K15-IGF1R^{KO}. (a) Experimental timeline. (b) Representative images of KO and WT male mice at the indicated time points (n = 3 vs 3). (c) Mean of representative timeline of hair follicle cycle after mifepristone treatment of WT and KO male mice (n = 3 vs 3). (d) Representative histology of back skin at the indicated time points (n = 3 vs 3), Scale bars: 100 µm in all micrographs.

Figure 3: Synchronized hair cycle shows delay in anagen/catagen stage switch. (a) Experimental timeline. (b) Representative images of KO and WT male mice at the different time points. (c) Time course of pigmented skin (n = 3 vs 3). (d) Representative histological pictures of dorsal skin from back at the different time points (n = 3 vs 3). (e) Hair type quantification in percent of total counted hairs (> 100 hair follicles per mouse) (n = 2 vs 6). (f) Hair cycle stage quantification in percentage of all counted hairs from nape skin at late time point (D20) (n = 2 vs 7). Mann-Whitney test, * $p < 0.05$; mean ± SEM.

Figure 4: MED1 expression and phosphorylation is altered in K15-IGF1R^{KO} animals. (a) MED1 mRNA level in plucked hair (n = 6 vs 4). (b) Western blot of MED1 in whole skin (n = 4 vs 4). (c) Western blot of phospho-MED1 in whole skin (n = 4 vs 4). Mann-Whitney test, *$p < 0.05$; mean ± SEM.

Figure 1

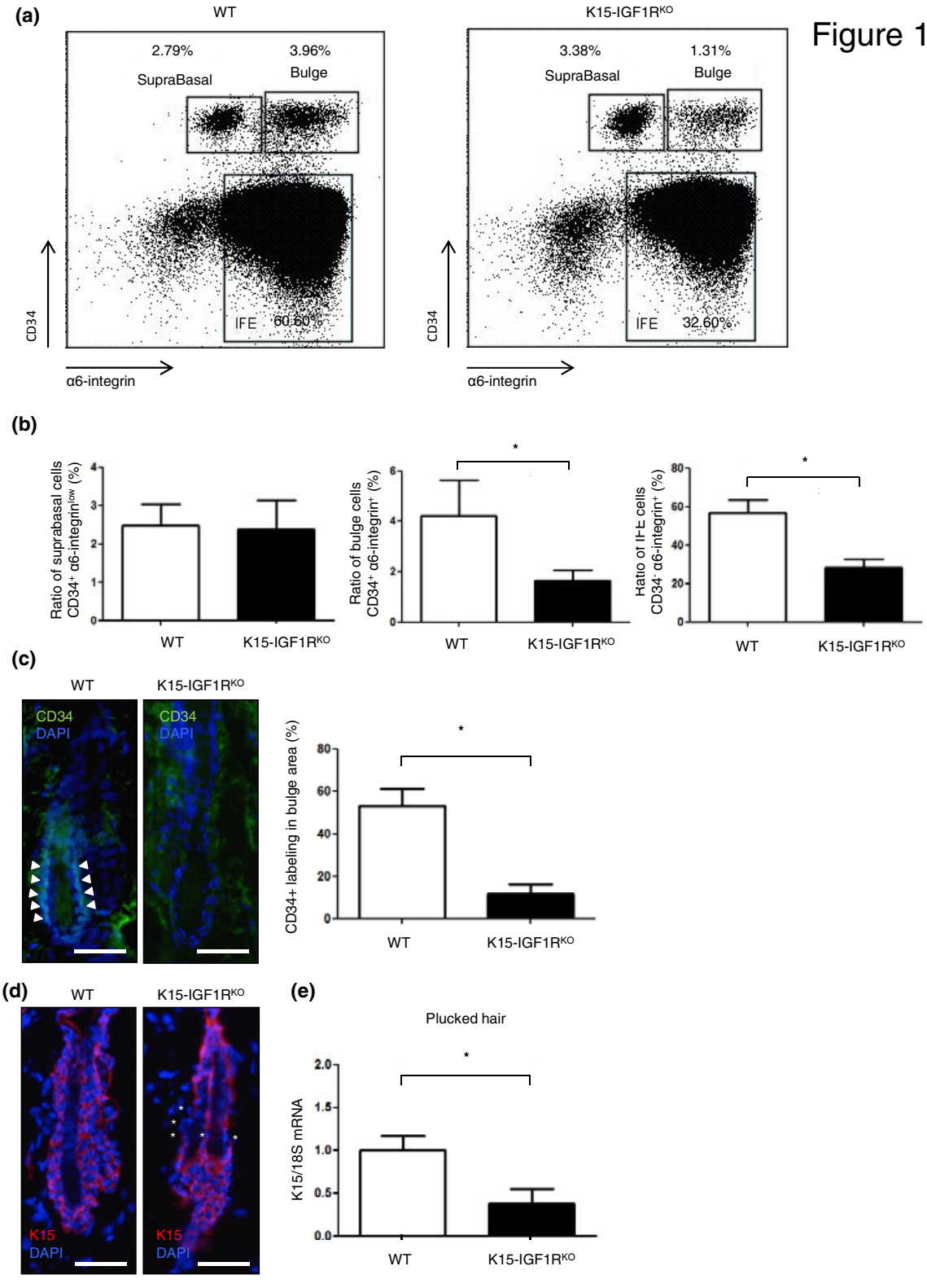

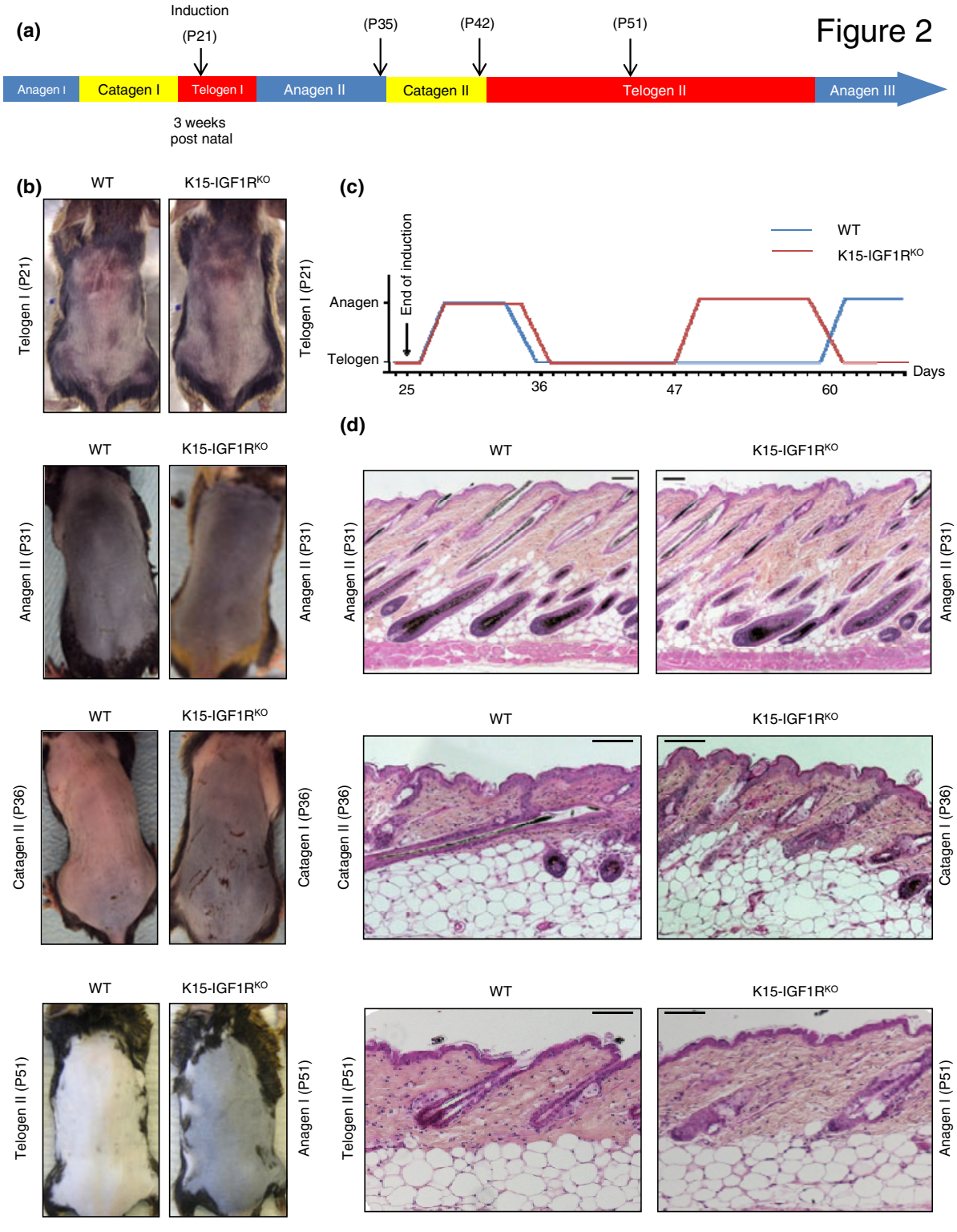

Figure 2

Figure 3

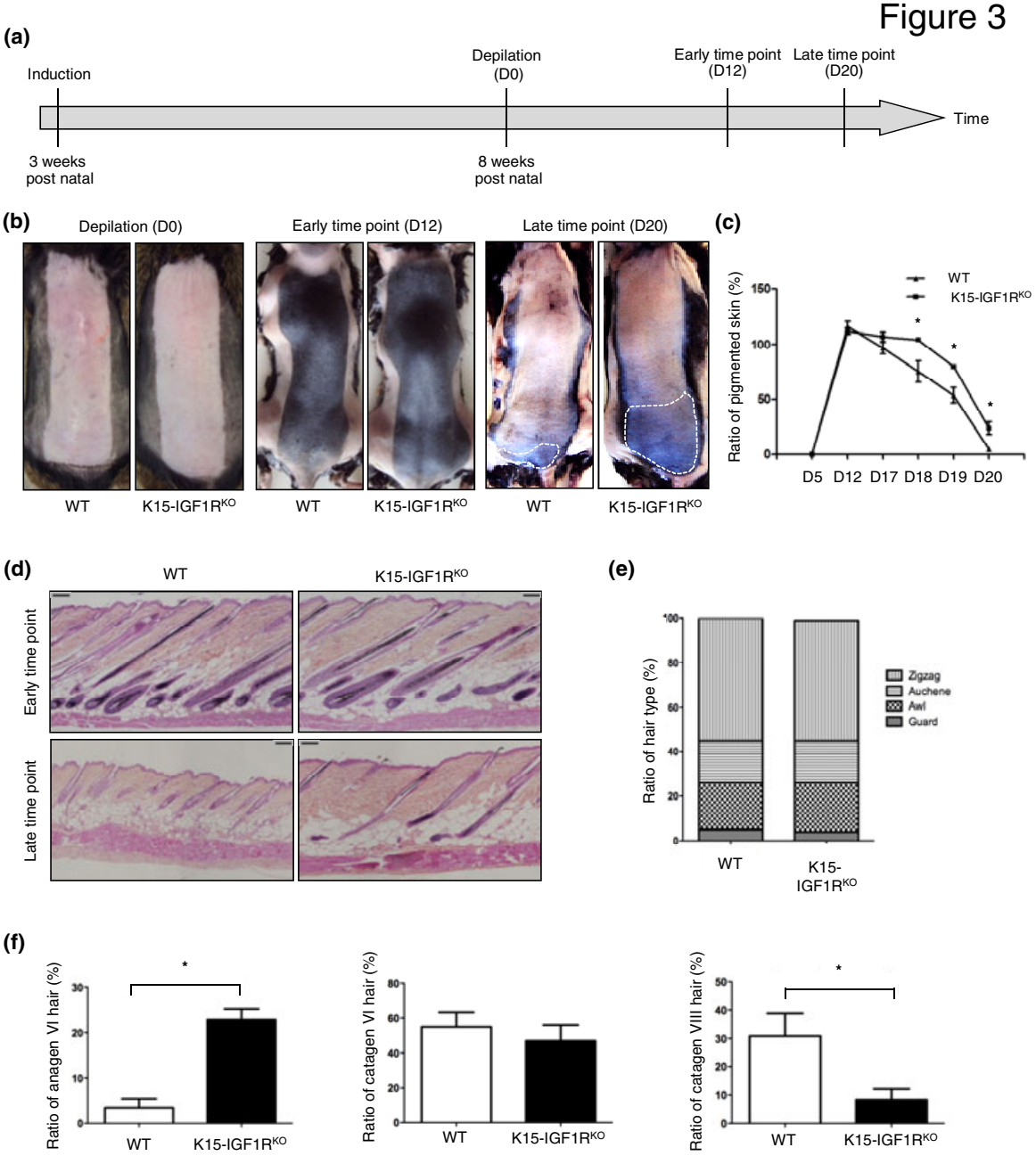

Figure 4